ELSEVIER

Journal of Power Sources 112 (2002) 531–546

JOURNAL OF POWER SOURCES

www.elsevier.com/locate/jpowsour

Analysis of battery current microcycles in autonomous renewable energy systems

A.J. Ruddell[a,*], A.G. Dutton[a], H. Wenzl[b], C. Ropeter[b], D.U. Sauer[c], J. Merten[d], C. Orfanogiannis[e], J.W. Twidell[f], P. Vezin[g]

[a]*Rutherford Appleton Laboratory, Chilton, Didcot, OX11 0QX Oxfordshire, UK*
[b]*TU-Clausthal, Leibnitzstraße 28, 38678 Clausthal-Zellerfeld, Germany*
[c]*Fraunhofer Institut für Solare Energiesysteme, Heidenhofstraße 2, 79110 Freiburg, Germany*
[d]*Trama TecnoAmbiental, Ripollés 46, E-08026 Barcelona, Spain*
[e]*ESCO, 122 Tatoiou, GR-14671 Athens, Greece*
[f]*AMSET Centre, Horninghold, LE16 8DH, England, UK*
[g]*Vergnet, 160 rue des sables de Sary, 45770 SARAN, France*

Received 12 December 2001; received in revised form 23 July 2002; accepted 16 August 2002

Abstract

Battery currents in autonomous renewable energy systems (RES) are generally predicted or measured in terms of mean values over intervals of 1 min or longer. As a result, battery charge–discharge cycles with periods less than the averaging period are ignored, and the actual battery ampere hour (A h) throughput and resulting battery wear may be seriously underestimated, leading to optimistic prediction of battery lifetime. This paper considers short charge–discharge cycles or microcycles, arising from the characteristics of autonomous renewable energy systems, including generators, regulators, loads, and load inverter. Simulation results are used to show that inverters operating directly from the battery can cause microcycles, resulting in significantly increased battery throughput. Initial experimental results of the effects of microcycles on battery capacity and charging characteristics, and the contributing processes, are discussed.

Keywords: Lead–acid battery; Cycling; Microcycles; Charge–discharge; Wind turbine; Photovoltaic systems

1. Introduction

The accurate prediction of battery lifetime in autonomous renewable energy systems is desirable in order to achieve reliable and economic designs, however there are many factors with complex interdependence making an accurate prediction difficult. Key operational issues affecting the battery lifetime are: (a) the system sizing for the particular operational conditions; (b) the operational temperature; (c) the operational control of charging, including the charge controller characteristics; and (d) the generation and load profiles. Methods of estimation of the battery lifetime in PV systems have been published by Spiers and Rasinkoski [1,2], Drouilhet and Johnson [3], and Symons [4]. The factors affecting lifetime may be broadly considered under two categories, the 'cycling lifetime', resulting from ampere hour (A h) throughput causing wear, and the 'float lifetime' resulting from processes during standby causing mainly positive plate corrosion. These lifetimes are defined for the two modes of operation (continuous cycling, or standby), and do not include the effects of additional acid stratification or irreversible sulphation that are likely to be caused by cycling at partial state-of-charge. Therefore, it is not surprising that the prediction of battery lifetime is frequently inaccurate, and the actual lifetime under the duty encountered in a real application is much shorter than anticipated.

A systematic definition by the Fraunhofer Institut Solare Energiesysteme (Fraunhofer ISE) of performance parameters for lead–acid batteries in renewable energy systems, identified four major classes of operating conditions based on battery currents and state-of-charge (SOC) cycles, and four classes of operating temperature conditions [5]. The battery current classification by Fraunhofer ISE is shown summarised in Table 1. The lifetime determining mechanisms resulting from a particular combination of operating

* Corresponding author. Tel.: +44-1235-445-551; fax: +44-1235-446863.
E-mail address: a.j.ruddell@rl.ac.uk (A.J. Ruddell).

0378-7753/02/$ – see front matter
PII: S0378-7753(02)00457-3

Table 1
Classification of battery operation conditions according to currents and state-of-charge cycles [5], where the storage size is in units of battery capacity divided by the mean daily load

	Class 1 (low currents)	Class 2 (medium currents)	Class 3 (medium currents)	Class 4 (high currents)
Cycles	Few cycles (mainly 1 per year)	Frequent partial cycles (at different SOC)	Frequent partial cycles (at high SOC)	Deep cycles (0.5–1 per day)
Typical storage size	>10 days	3–5 days	1–3 days	1 day

conditions, such as battery throughput, state-of-charge profile, and temperature profile, are likely to be similar within classes. This suggests that data obtained from monitoring battery currents and temperatures, together with the observed battery lifetime, could be used by system designers to improve prediction of battery lifetime. The approach would require simulation of a proposed new system, and comparison with existing data in the same class.

In most applications, batteries are clearly in either charge or discharge mode of operation. However in renewable energy systems (RES), the generators and loads often operate concurrently, and therefore superimposed fluctuations result in battery current amplitude changes and polarity reversals, leading to short-term charge–discharge cycling [6]. This paper describes analysis of the additional throughput due to 'microcycles', defined as polarity reversals of the battery current with periods less than minutes. The charge and discharge currents encountered by batteries in renewable energy systems varies widely according to the application. Usually, there are daily and seasonal cycles, as well as operation for extended periods at intermediate SOC. In order to facilitate analysis, the battery charge and discharge currents may be recorded, or obtained by computer simulation, as mean currents over a sampling interval. The data sampling interval is usually not less than 1 min for long-term data, and is frequently much longer. This means that computation of the battery ampere hour (A h) throughput will be underestimated when there are battery current polarity reversals during the averaging interval. This paper describes analysis of battery throughput in two typical RES installations. The investigation concentrated on estimating the short-term charge–discharge cycle which can be caused by the variability of the renewable energy resource or the load demand, or by power electronic inverters causing ac components in battery currents. Typically the battery microcycle throughput will be largest during periods when the level of power generated by the renewable energy sources is approximately equal to the load. Experimental results indicating that such short-term current fluctuations have a detrimental effect on battery performance have been published elsewhere [7]. These results indicate that microcycles cause acid stratification and battery wear, resulting in reduced capacity and possibly reduced lifetime.

Assessment of the magnitude and effect of microcycles has received little attention in the literature, and there are only a few papers which describe experiments on the effect of frequent changes of current direction in the range from 0.1 to 50 Hz and beyond. Batteries used in uninterruptible power supply (UPS) applications are continuously float charged, and may be subjected to 100 Hz ripple from the mains rectifier. It is well established that this causes no battery degradation as long as the RMS battery current is less than $0.05 \times C_{20}$ during float operation. However, Harrison [8] reported potential problems where a battery is subjected to high frequency shallow cycling (HFSC) at high battery SOC, where the coulombic efficiency during charging is low. The application of equal charge and discharge currents in addition to a small dc current to offset self-discharge could result in the battery being progressively discharged to around 70–80% SOC, where the charge efficiency approaches 100%. König [9] describes a set of experiments using superimposed currents at 16.67 Hz, a frequency used in German railways. It was found that the electrode connections of deeply discharged batteries rapidly corroded, when the batteries were subject to microcycles at 16.67 Hz. Corrosion was not detected at any SOC when microcycles were not present. König suggested that the high corrosion was due to very high current density in areas where there was no lead sulphate to interrupt the current path.

It is also worth mentioning research into the effect of fluctuating currents, even when these do not include polarity reversals. The reported results of papers published on the effects of ac currents, such as pulse charging, or rapid charge–discharge cycling, appear to be contradictory. For example, Lam et al. [10] claims that an increase in cycle life by a factor of 3–4 can be obtained by rapid pulse-charging, while Ozazaki et al. [11] claims that the influence of ac superimposition on the charging current has a negligible effect on cycle life.

The ageing of batteries in autonomous power supply systems is due to a large number of effects. Acid stratification, inadequate charging strategies, deep discharge, cell individualisation in strings, insufficient maintenance, long periods in deep states of charge, and inappropriate battery choice for a given system, are the main reasons for short lifetimes. Within the joint research of the authors, including economic analysis, a range of measures to extend battery lifetime (better charging strategies, charge equalisers for long strings, deep discharge protection based on state-of-charge determination, and electrolyte agitation systems) have been identified and quantified. However, this is not the focus of the work presented in this paper.

2. Battery currents in renewable energy systems

Superimposed ac currents (due to the rectified ac output from a wind turbine generator, and PWM series regulation of PV generator output, and inverters driving loads) can cause rapid fluctuations, and in certain cases, polarity reversals, of the battery current. In a particular time interval, the battery current can be considered to consist of a mean or dc value, together with a spectrum of frequencies that cause no net flow of current when integrated over time. If the ac current is of a sufficiently high frequency and low amplitude, the ac current can be supplied by the double-layer capacitance, represented by the charge distribution at the electrode–electrolyte interface (Helmholtz layer), while at low frequencies the current is supplied by corresponding levels of electron-transfer. This simple explanation suggests that high frequency currents (for example >1000 Hz) may not cause changes in the electrode materials, even when the net battery current has polarity reversals, and therefore may not result in battery wear. On the other hand, low frequency currents utilise active material. The authors are not aware of any investigations into the relative levels of current supplied by the double-layer capacitance and by electron-transfer, as a function of ac frequency and amplitude. However, it is clear that the net utilisation of active material remains proportional to the mean current if the net battery current does not have polarity reversals, while a low frequency ac component with peak larger than the mean value causes polarity reversals of the net battery current, and charge–discharge cycling of the active material, resulting in increased battery wear.

Typically the size of RES components are designed using calculations of energy balance over a daily or monthly time interval, and simulation for long periods is rarely done with data averaged over periods less than 1 min. Therefore, charge–discharge cycling with periods shorter than the averaging period is ignored, the battery throughput is underestimated, and the predicted lifetime is optimistic.

A more rigorous determination of the battery current in a particular application would produce a more accurate estimate of the total battery throughput, and result in a more accurate prediction of battery lifetime. Therefore, it is proposed in this paper that relatively fast time-series data of the battery current, obtained by simulation or by measurement, can facilitate analysis of the ac components caused by the generators, regulators, and loads in a particular application. Spectral analysis of measured data with a short time-step would be useful to reveal the presence and the frequencies of fast battery current microcycles. Note that several components of the power system are non-linear (e.g. wind turbine, charge regulator, battery), and therefore, analysis of the charge and discharge currents is best done in the time-domain.

A further effect of additional charge–discharge cycling is reduced system efficiency. At battery SOC >80% the coulombic efficiency during charging is progressively reduced, and in large capacity systems designed for many days of autonomy, inefficient shallow cycling at high SOC may prevent the battery from ever becoming fully charged. This effect will be more pronounced when the average generated input is less than or only marginally greater than the average load output, a situation which can arise in PV systems in winter, and which can lead to a progressive walk-down in battery SOC. Although this effect has not been analysed in this paper, it could be included by modelling the charge efficiency as a function of battery SOC using charge efficiency models described by several authors [12–14].

The battery temperature has a significant impact on lifetime, and is influenced by three major factors, i.e. ambient temperature, battery housing and charge–discharge cycles. Increased temperature has a negative impact on lifetime due to corrosion and drying out of batteries (rule of thumb: the lifetime is halved for a temperature increase of 7–10° K). Other ageing effects which are of relevance in autonomous power supply systems have a complex correlation with temperature. For example, reversal of sulphation during charging is easier at higher temperatures, whereas the formation of large sulphate crystals during discharge is accelerated at higher temperatures. Therefore, the impact of battery temperature on lifetime is highly dependent on the operating conditions, and is difficult to quantify.

2.1. Photovoltaic (PV) and wind turbine generator currents

Battery current fluctuations in a renewable energy system can be caused by the generator and the regulator characteristics, as well as by the renewable source. Wind speed fluctuates rapidly due to turbulence, and wind turbine output power is a non-linear function of wind speed cubed, modified by the machine dynamics, and subject to the rated power limitation. Therefore, the output of wind turbine generators show considerable fluctuations at frequencies up to several Hertz. On the other hand, the solar irradiance generally changes slowly, being mostly associated with cloud movement and the daily periodicity. The output of PV modules is a nearly linear function of the solar irradiance, and spectral components of PV generator currents without the effects introduced by charge regulators are therefore, usually at low frequencies <0.1 Hz.

In large photovoltaic (PV) or PV/wind hybrid systems, the PV generator is connected via a dc–dc converter, which usually includes maximum power-point tracking (MPPT). The wind generator ac output is rectified to dc, and may be followed by a dc–dc converter, depending on the size of the wind turbine. Battery current microcycles may result from high frequency noise from the power electronics converters, however, most of this can be easily removed by filtering.

Small systems (for example <1 kW generating capacity) have additional microcycles resulting from the simple direct connection method of the generators to the battery, without using dc–dc conversion. Pulse-width modulation (PWM) of the PV generator current is used to regulate charge current in

the constant voltage 'taper charge' or 'float charge' modes, when the battery approaches full charge. The PWM waveform is controlled in various ways, for example, the battery voltage may be operated within limits by controlling the on and off switching times, resulting in a variable frequency PWM waveform; or a fixed frequency may be used (e.g. 8 Hz) with a variable duty cycle. This results in a pulse charging current, and microcycles can occur when the load current is less than the PV generator peak current. On the other hand, linear shunt regulators, generally used only in very low power systems, divert current from the battery in an analogue fashion, and do not cause microcycles.

In the case of a small wind turbine with a permanent magnet generator, the rectified ac output from the wind turbine generates pulsed currents at amplitudes and frequencies which depend on the rotor and wind speeds.

2.1.1. Experimental monitoring

The pulsed charge–discharge currents in a small PV/wind system were investigated experimentally. The system used consists of a PV generator (2 × 60 Wp panels, facing south, at an inclination 65° to the horizontal), a wind turbine (Marlec FM910 Windcharger, rated at 50 W @ 10 m/s, mounted at 6.5 m above ground level), a deep cycle battery (12 V, 230 A h capacity @ 100 h rate), together with charge regulators, a computer-controlled load, and a monitoring and logging system. The Marlec FM910 is typical of small battery-charging wind turbines, and the permanent magnet single-phase ac generator output is full-wave rectified and supplied to the battery via a shunt regulator. The wind turbine rotor speed, and the generator output frequency, are directly related to the wind speed and the electrical load on the generator. This system was designed to supply a load of up to 30 A h per day with a maximum of 5 days autonomy for 70% depth of discharge (DOD). This system is class 1, according to the Fraunhofer ISE classification [5], and is used at the Rutherford Appleton Laboratory (RAL) test site for different types of investigation. A PC with LabVIEW software was used to acquire several channels of data at 1 ms sample intervals. The sampled data included instantaneous values of PV current, wind turbine current, battery charge and discharge current, load current, battery voltage, battery temperature, solar irradiance, and solar cell temperature.

The sum of instantaneous currents at the bus-bar of an autonomous power system is zero, as expressed by the relation

$$I_{pv} + I_{wt} = I_{reg} + I_b + I_l \quad (1)$$

where I_{pv} and I_{wt} are the PV and wind turbine generator currents, respectively; I_{reg} the shunt regulator current; I_b the battery current (positive = charge) and I_l is the load current.

The time series of a 16-s period of operation was acquired, where the PV generator current I_{pv} was zero, the wind turbine generator current I_{wt} was fluctuating rapidly due to wind turbulence, and the load current I_l was constant 3 A. The battery was not fully charged, therefore, the shunt regulators were inactive (I_{reg} was zero), and the battery current was equal to the full available generator current less the constant load current, and with equivalent fluctuations.

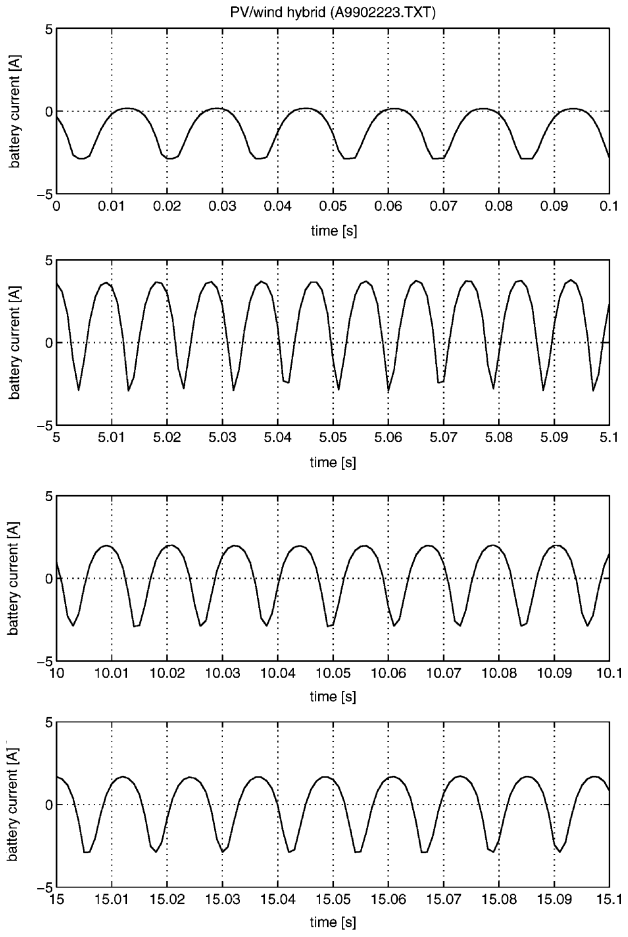

Fig. 1. Measured instantaneous battery currents at various times within a 16-s interval, caused by a wind turbine generator.

The detailed battery current fluctuations are illustrated in Fig. 1 where four 0.1-s periods of operation have been selected from the complete 16-s acquisition. It can be observed that the battery current consists of full-wave rectified pulses covering a range of frequencies, with a bias according to the instantaneous operating conditions, and with amplitude and frequency increasing with wind speed. The result is that the battery can be subject to rapid charge–discharge reversals, as illustrated during the periods of operation in Fig. 1b–d. Note that with zero input from the wind turbine, the battery current would supply the load, and would be equal to −3 A (discharging).

The power spectral density (PSD) estimate of battery current for the complete 16 s data-set is shown in Fig. 2. The PSD shows the spectral components of the fundamental component of the rectified ac output, in the region 60–100 Hz, resulting from variable speed operation of the wind turbine during the short measuring period.

It should be noted that most permanent-magnet battery-charging wind turbine generators with powers greater than

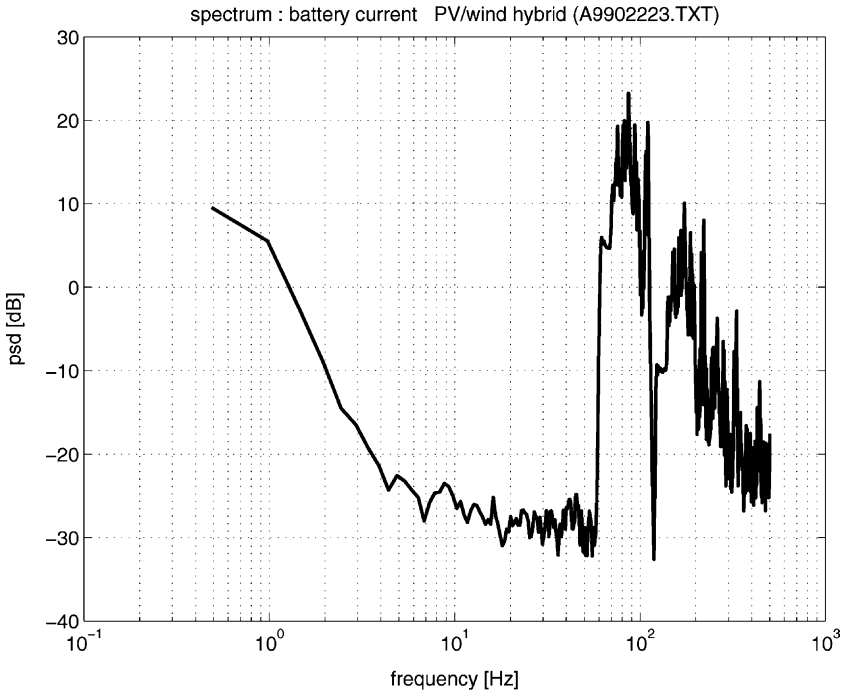

Fig. 2. Power spectral density estimate of battery current, for a 16-s acquisition.

100 W are three-phase. In theory, the instantaneous power into a linear load would be constant, however, the combination with a non-linear battery load will also result in pulsed battery currents.

2.2. Load currents

The topology of the power electronics inverter supplying the ac network is important for the analysis of throughput caused by microcycles. Small to medium-sized systems often have a maximum 48-V battery bank for safety reasons, and because of the available standard cell capacity. In this case, the simplest power electronics topology consists of a single-stage dc–ac inverter, followed by a transformer to produce the required ac network voltage at 50 or 60 Hz. Large systems may have a battery bank voltage greater than the peak ac voltage, when a PWM inverter can be used to produce the ac network voltage directly. The attractiveness of this topology is its simplicity, however, there is a drawback. The current on the dc side (battery) of a single-phase PWM inverter can be analysed[1], and it is found that currents drawn from the battery will include an ac component at twice the inverter output frequency (i.e. at 100 or 120 Hz), with amplitude dependent on the load power factor (p.f.), as shown for constant real power in Fig. 3. There will also be high frequency switching components, not shown in Fig. 3, which can easily be removed by filtering. These examples show that when the load is supplied by the battery alone, microcycles occur when the load power factor is less than unity. Non-zero generator currents will change the bias of the load current cycles, which will change the microcycle throughput. Note that in Fig. 3, the dc side (battery) current is viewed as the inverter input, therefore, the convention in this case is 'positive current = battery discharge'.

The additional battery throughput Coulombs (C, A s) for a single microcycle may be evaluated as

$$C_{\mathrm{m}} = \int_{t0}^{t1} |I_{\mathrm{b}}| \mathrm{d}t \tag{2}$$

where I_{b} is the battery current consisting of a mean value with superimposed microcycle; $t0$, $t1$ are the times of the battery current zero-crossings; and the modulus ensures that C_{m} is positive. This expression assumes that a superimposed microcycle which causes an additional charge, also causes a corresponding additional discharge. However, no account is taken of the reduced charge efficiency at high SOC, which may result in progressive discharge, or 'walk-down'.

An equivalent expression, which avoids the need to evaluate the zero-crossings for each microcycle, can be used to evaluate the additional throughput for a microcycle with period T seconds

$$C_{\mathrm{m}} = \frac{1}{2}\left[\int_0^T |I_{\mathrm{b}}| \mathrm{d}t - \left|\int_0^T I_{\mathrm{b}}\, \mathrm{d}t\right|\right] \tag{3}$$

where the second term is simply equivalent to the absolute value of the mean current multiplied by the period T. The factor 1/2 reflects that the additional throughput is evaluated

[1] N. Mohan, T.M. Undeland, W.P. Robbins, Power Electronics: Converters, Applications, and Design, Section 6.3, Single-Phase Inverters, Wiley, New York, 1989, pp. 114–129.

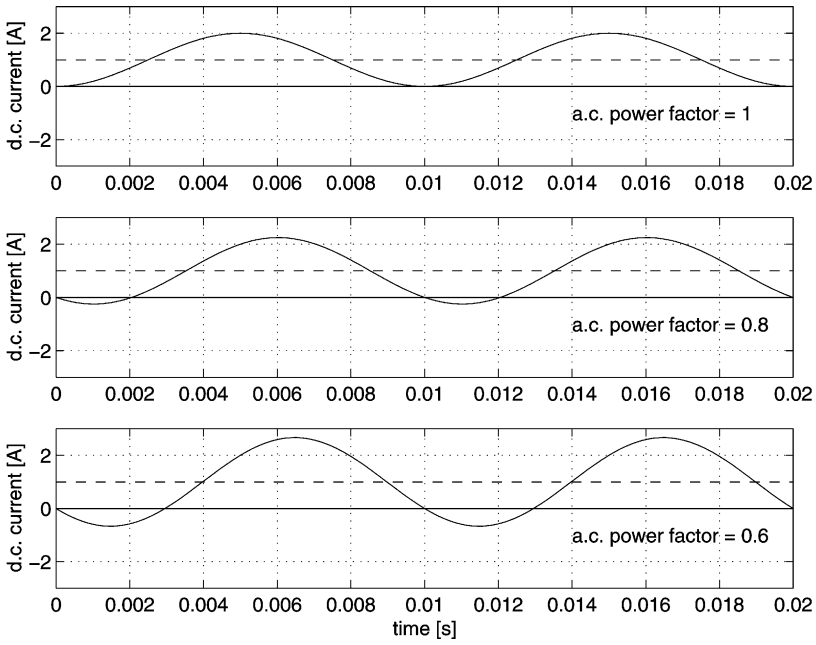

Fig. 3. Calculated dc side current in PWM inverter supplying a 50-Hz load at various power factors and constant real power (positive: current into inverter).

as additional discharge only. The battery throughput in Coulombs (A s) per second is then C_m/T, which is numerically equivalent to the usual units of Ah h^{-1}.

Examples of waveforms are illustrated in Fig. 3. During periods when the current waveform does not have a zero-crossing, as shown in Fig. 3(a), the calculated microcycle throughput is zero. However, when the current waveform has zero-crossings, as shown in Fig. 3(b and c), there is an additional microcycle throughput, which in this case is caused by charging. Calculation of the additional charge using Eqs. (2) or (3) shows the battery throughput is increased by 3.4% for p.f. = 0.8, and by 12.9% for p.f. = 0.6.

In renewable energy systems, the generator current has the effect of applying a bias to the battery current, reducing the mean battery discharge current. The battery may be viewed as being charged (or discharged) by the mean current, while the superimposed ac component caused by the load inverter causes additional throughput due to microcycles. The effect of a steady PV generator current, is illustrated in Fig. 4, where the maximum microcycle throughput occurs when the generator current is equal (+1 A in this case) to the mean battery current due to the load (−1 A in this case), and increases as the load power factor is reduced. It is clear that there is always some microcycle throughput caused by a single-stage inverter when the generated current is less than twice the mean load current. In the usual case where the generator and load currents are time-varying, a calculation based on the time-series data is required to estimate the battery throughput based on the mean currents at each time-step, and the additional throughput due to microcycles.

An alternative topology consists of a dc–dc converter operating at a high switching frequency, feeding a dc link, and followed by a dc–ac inverter to 230 V ac. The high frequency currents drawn by the dc–dc converter from the battery can be easily removed by filtering. Proper operation of the inverter requires a dc link voltage in excess of the peak ac voltage (for a 230 V ac supply, the peak ac voltage is 325 V, and the dc link voltage is 400 V, for example), and with a low ripple. Therefore, the dc link should have sufficient capacitance to ensure low ripple voltage. The use of this topology makes it possible to reduce the ac currents drawn from the battery, however, the hardware may be more expensive than a single stage dc–ac inverter.

3. Estimation of battery throughput

3.1. Simulation procedure

Computer simulation is a cost-effective method of investigating the battery operating regimes of renewable energy systems in the various classes, including variables such as system size and configuration, energy supply, and load profiles. A simple simulation model has been developed using Matlab and Simulink. The model was first used to investigate the battery state-of-charge (SOC) during a 1-year period of operation with 1-h time-steps. The design or simulation of a solar energy system requires information about the solar radiation and the ambient temperature; and in the case of a PV/wind hybrid system, the wind speed. Therefore, solar and wind resource data with a suitable time-step must be obtained, and the inputs to the PV and wind generators estimated, taking account of their orientation and position. A convenient simulation time-step is 1 h, when hourly mean irradiance data (W m^{-2}) may be used.

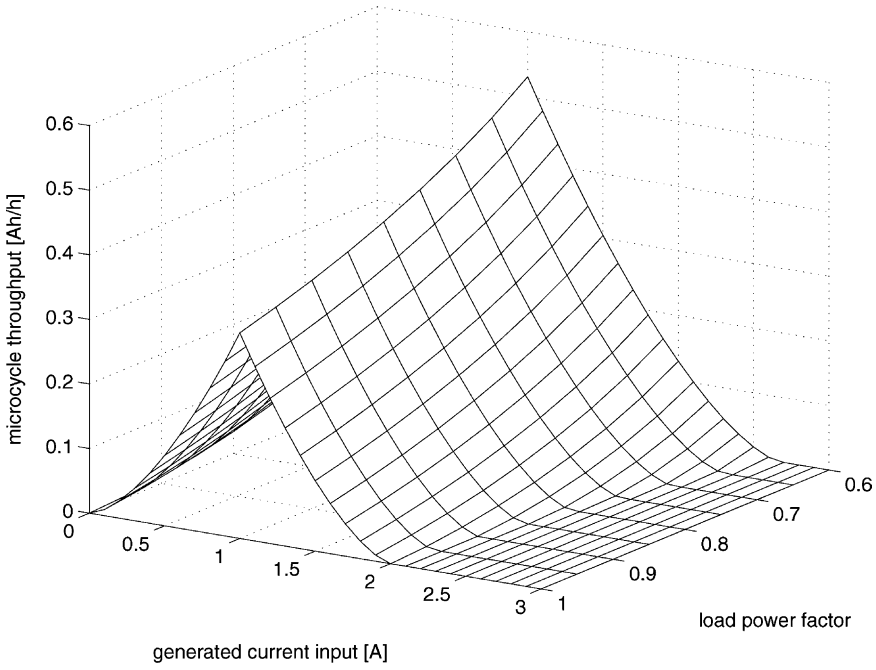

Fig. 4. Calculated additional battery throughput due to microcycles, for a load inverter mean current of −1 A. (positive: current into battery).

Similarly, the wind speed at each time-step is assumed to be equal to the mean speed during this hour. A data-set of 1 year of weather data with a time-step of 1 h was obtained for southern England, and the data were processed using a standard procedure.

The simulation procedure can be illustrated using the small PV/wind system defined in Section 2.1.1. The simulation was run for a period of 1 year, with a daily load profile consisting of 1 A (00:00–19:00 h); 2 A (19:00–22:00 h); 1 A (22:00–24:00 h), resulting in a total load of 27 A h per day. The additional evening load tends to promote battery cycling due to the relative timing of the load and PV generator currents. The inputs to the simulation model are the meteorological time series data including solar irradiance and wind speed, and the outputs from the model are the generator currents, the battery current, and the battery SOC. The currents available from the wind and PV generators are shown in Fig. 5, however, when the battery is fully charged, the current supplied to the battery will be regulated. The simulated battery current and SOC are shown in Fig. 6 (simulation for a period of 1 year), and Fig. 7 (simulation for a period of one month). The characteristic 'winter' effect can be observed, where the battery SOC is generally at a low level. No loss of load events occurred, although operation at such low levels of SOC would be undesirable from the point of view of supply security, as well as for the battery lifetime.

3.2. Microcycles

By our definition, *microcycles are polarity reversals of the battery current with periods less than minutes*. Analysis of microcycles would require data to be acquired at a sampling frequency up to say 1 kHz, and the analysis over a long operating period (e.g. 1 year), would require a large quantity of data. Such data are not generally available and even in the test installation are not routinely recorded. Therefore, it was proposed that data with a time-step of 1 h, obtained by simulation or by measurement, should be used to define the mean currents, and then a typical waveform for the battery ac current caused by the generators and the load calculated in each time-step. This would allow estimation of the microcycles over a long period.

The first stage was to analyse the 1 h time-series data. To illustrate the procedure, part of the simulation results already shown in Figs. 5–7, has been analysed and plotted. The PV generator, wind turbine generator, load, and battery currents for a 10-day period are shown in Fig. 8(a–d) respectively, and 35 battery current microcycles are observed. The battery charge input and discharge output are 91.8 and 125 A h, respectively.

The next stage in the analysis is to include the fast battery current fluctuations caused by wind turbulence, and the inverter supplying the load. Several simplifying assumptions were made to facilitate estimation of the additional microcycle throughput.

(a) The analysis is based on simulation results with 1-h time-step. The effects of wind power fluctuations and load inverter ac currents are included by superimposing ac currents on the 1-h mean battery current at each time-step.
(b) The battery coulombic charge efficiency is assumed to be 100%, and superimposed microcycles with equal A h charge and discharge are assumed to have no effect on the battery SOC profile. In practice when the battery

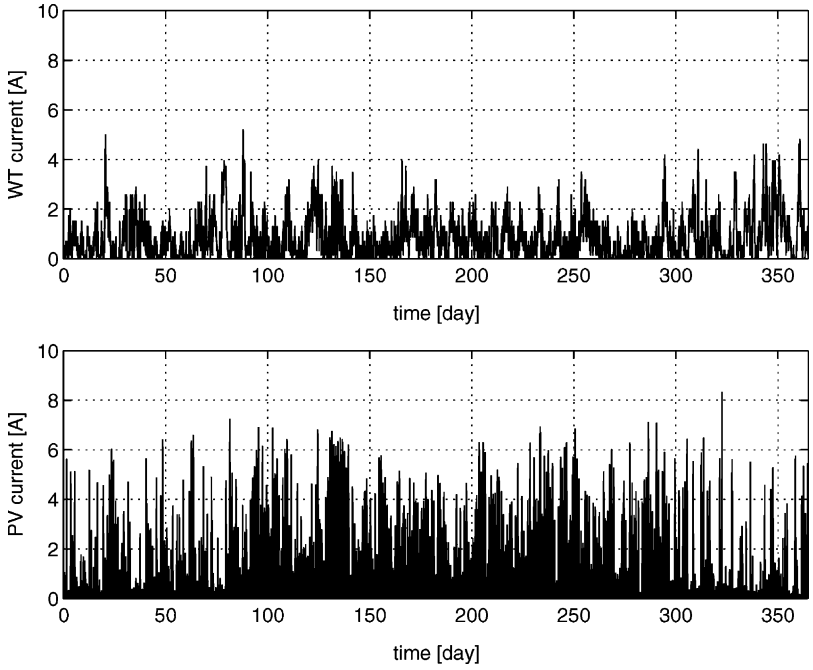

Fig. 5. Simulated currents available from wind turbine and PV generators for a period of 1 year (class 1 system).

SOC is in the region above 80%, the coulombic charge efficiency reduces progressively to 10% or less. Therefore, even when the mean current is zero, microcycles at high SOC would result in a progressive 'walk-down' of battery SOC to around 80%. Therefore, microcycles can result in a loss of overall system efficiency, and a generally lower battery SOC profile.

(c) The battery self-discharge current at open circuit conditions, typically less than $0.002 \times I_{100}$ (resulting in 1–2% capacity loss per month at 20 °C and approximately 2.1 V per cell), is assumed to be negligible compared with typical operational currents.

(d) The PWM inverter high-frequency switching components are assumed to be removed by filtering—this is relatively easy, and is standard practice in order to satisfy electromagnetic (EMC) regulations.

(e) Only linear loads, with variable power factor and the same real power, are considered. The shape of the

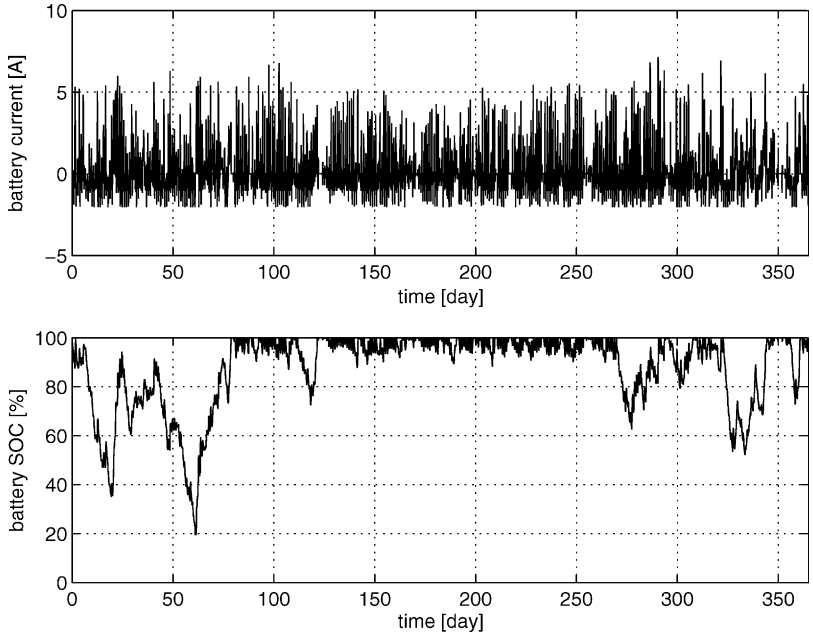

Fig. 6. Simulated battery current and SOC for a period of 1 year (class 1 system).

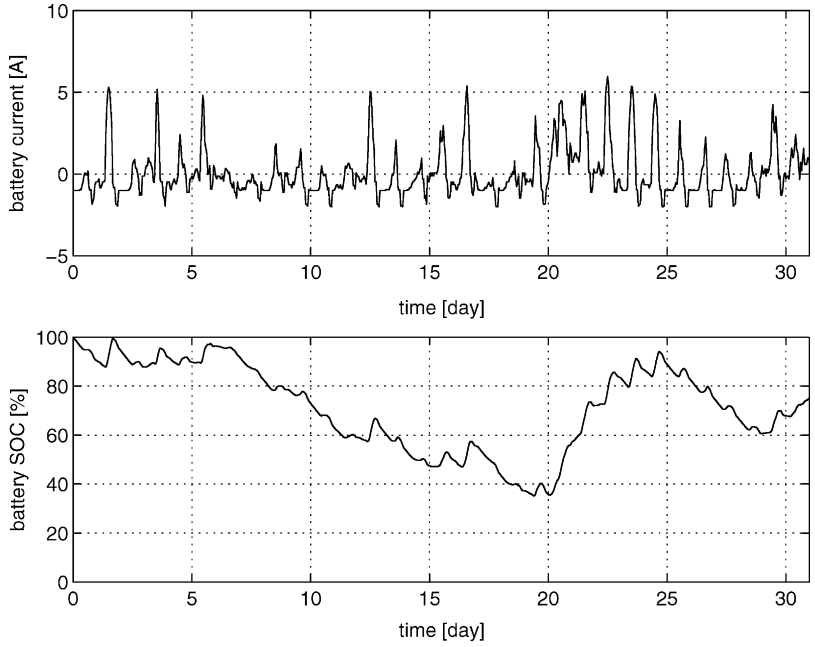

Fig. 7. Simulated battery current and SOC for a period of one month, i.e. days 1–31 of Fig. 6 (class 1 system).

current waveform is affected by load non-linearity. Assessment of the effect on microcycle throughput and the effect on battery lifetime would require further analysis.

(f) A parameter called 'ripple attenuation' is used to specify the capability of the load inverter to isolate the battery from the ac load waveform. A ripple attenuation of zero represents the case where the PWM inverter operates directly off the battery, without any intermediate energy storage. Where the battery voltage is relatively low (e.g. 48 V dc), the inverter may be followed by a transformer to produce a suitable ac supply (e.g. 230 V ac). In this case, the current drawn by a single-phase 50 Hz inverter from the dc side has a large component at 100 Hz. The effect of capacitance in the dc link of a two-stage inverter may be represented by increased ripple attenuation.

(g) The analysis assumes a wind power waveform, which includes the effect of wind turbulence, but excludes the effect of the rectified ac generator output. Inclusion of

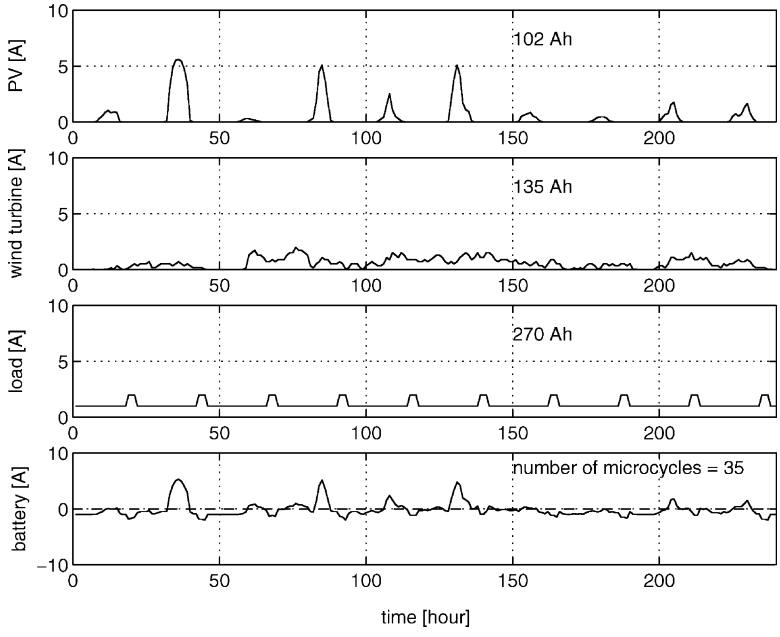

Fig. 8. Simulated generator, load, and battery currents for a period of 10 days, i.e. days 1–10 of Fig. 7 (class 1 system).

the effect of the rectified current pulses is possible, by including the wind turbine speed and the non-linear current waveform in the model, however, this would require much simulation time.

(h) A typical wind speed time-series of an operating wind turbine was acquired with a sampling frequency of 100 Hz for a period of 10 s (1000 samples). This time-series, together with the wind turbine power curve, was used in a series of transformations to produce a wind power time-series corresponding to the mean wind power at each 1-h time-step. This time-series was then used to estimate the battery current fluctuations in each 1-h time-step.

3.3. Analysis of a class 1 system

A practical example of a small PV/wind system, as described in Section 2.1.1, was used for analysis. An example of the synthesised 10 s waveform for a single 1-h time period (hour number = 65, i.e. 17:00 h on day 2) is shown in Fig. 9, where the mean PV generated current is zero, the mean wind turbine generated current is 1.08 A, the mean load current is 1 A, and the mean battery current is 0.08 A. The load power factor is assumed to be unity, and the ripple attenuation of the load inverter is assumed to be zero. The envelope of battery current fluctuations caused by the load inverter is shown dotted. In the 10-s period, the number of microcycles caused by the wind turbine generator is only five, while the number of microcycles caused by the load inverter is 1000. Although this illustrates only one short period of simulated operation, it seems obvious that the microcycle throughput caused by the load inverter is much greater than that caused by the relatively smooth output from the wind turbine generator. This is confirmed by analysis of the additional microcycle throughput for a short period of 10 days, with the results summarised in Table 2.

Table 2
Additional battery throughput resulting from load inverter and wind power fluctuations

Battery A h discharge, without microcycles	124.7
Microcycle A h caused by load inverter only	25.3
Microcycle A h caused by wind power fluctuations only	1.3
Microcycle A h caused by load inverter and wind power fluctuations	26.1

The system was simulated for a period of 1 year, to investigate the effect of ripple attenuation and load power factor on the additional battery throughput caused by the load inverter. The results are summarised in Table 3.

The specified endurance of the VRLA battery is 500 cycles according to IEC 896-2, where each discharge is 3 h @ $2 \times I_{10} = 114$ A h ($C_{10} = 190$ A h, $I_{10} = 19$ A), giving a

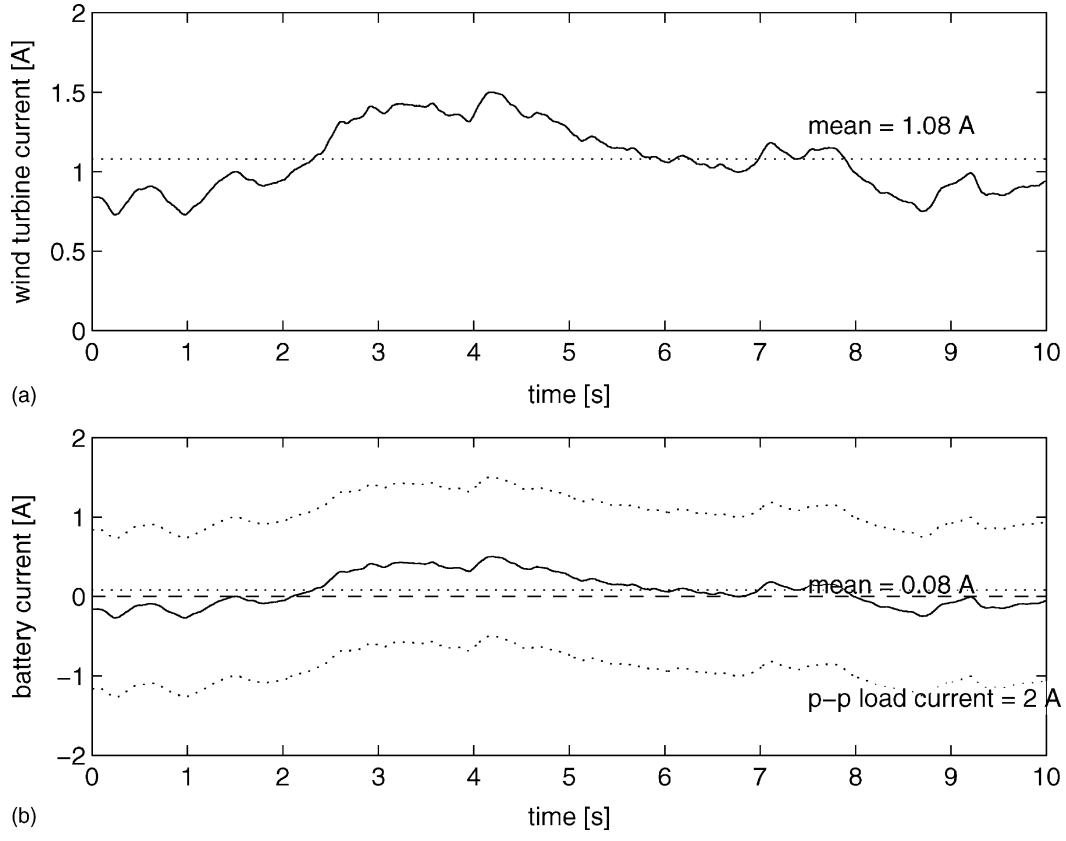

Fig. 9. Simulation of fast fluctuations in battery current, for a 10-s period during hour number 65 of Fig. 8, showing: (a) the wind turbine generator current, and (b) the battery current with the envelope of load inverter current (class 1 system).

Table 3
Summary results for the class 1 system, showing the additional throughput caused by microcycles, at different load factors and ripple attenuation

Ripple attenuation (%)	Load power factor	Total A h per year
100	1–0.6	3510
0	1	4620 (+32%)
0	0.6	6175 (+76%)

total A h discharged over the whole cycle life of 57,000 A h. The currents in the class 1 system are much smaller than I_{10} and generally of the order of I_{100} ($C_{100} = 230$ A h, $I_{100} = 2.3$ A), however, the total A h delivered by the battery is assumed to be independent of the currents but dependent on the max. DOD only, and defines the lifetime at various discharge rates [1]. The additional A h throughput caused by microcycles is likely to reduce the lifetime of the battery, however, neither the magnitude of such a lifetime reduction nor the mechanisms are fully understood. It is a reasonable assumption that the additional throughput caused by microcycles is simply added to the conventionally measured throughput for the purpose of lifetime estimation. The assumption that lifetime is only determined by throughput would give an optimistic prediction of battery lifetime in the simulated system, where including the throughput due to microcycles, a cycling lifetime of over 9 years (57,000/6175) would be indicated. In this case, the currents are small and it would take many years to reach the maximum capacity turnover defined by the IEC cycle endurance test, and it may be assumed that the primary limit to battery lifetime is its float lifetime, specified as 5 years for this VRLA battery. The float lifetime is mainly governed by corrosion processes, which are almost independent of currents but depend on electrode voltage, temperature, and state-of-charge (acid concentration). In this example, no significant lifetime reduction by microcycles would be expected, as the capacity throughput is low and is not the primary limit in determining the end of life.

3.4. Analysis of a class 2 system

TramaTechnoAmbiental (TTA) has installed approximately 400 PV installations in northern Spain on behalf of the SEBA users association, and provided monitored data for 1999 for a typical ‘mountain refuge’ system. The mean battery current was measured at each 1-h time-step, and does not have to be obtained by simulation. The system operation is class 2 according to the Fraunhofer ISE classification, with 1350 Wp PV and a 48 V, 735 A h battery. The battery type is flooded cell with tubular positive plates, giving a long cycle life, specified by the manufacturer as 1000 cycles @ 75% DOD, giving a total A h discharged over the whole cycle life of 551, 250 A h. The standby lifetime at a float voltage of 2.3 V per cell is around 12 years @ 20 °C.

The time-series of operation for a 10-day period is shown in Figs. 10 and 11, while the results for a period of 1 year are summarised in Table 4. The effect of the load power factor and the inverter characteristics on throughput are shown in Figs. 12 and 13.

The assumption that lifetime is only due to total throughput would give a very optimistic prediction of battery lifetime in this system, where including the throughput due to microcycles, a cycling lifetime of around 28 years (551, 250/19, 220) would be indicated. However, a calculation of

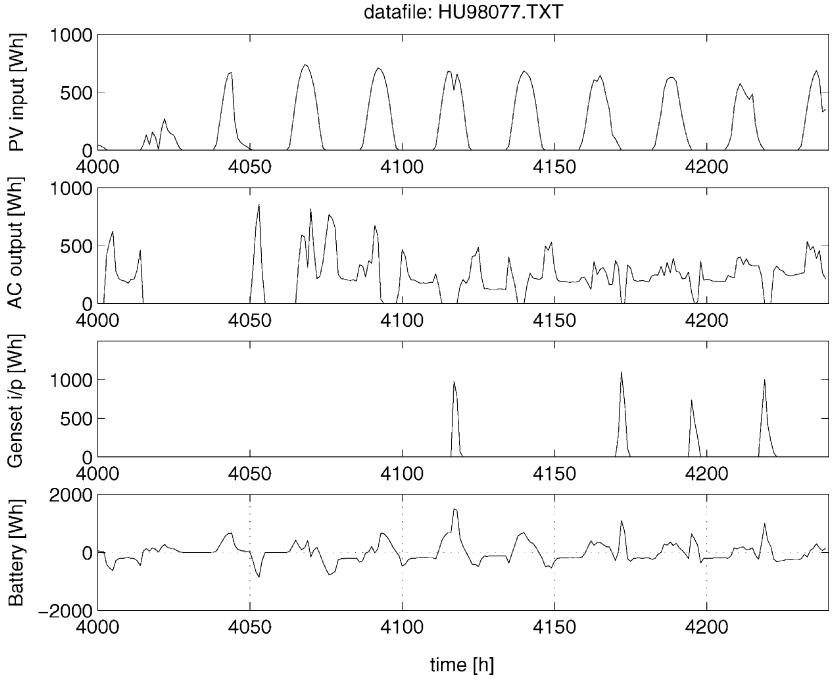

Fig. 10. Energy flows for a 10-day period (TTA’s ‘mountain refuge’ system).

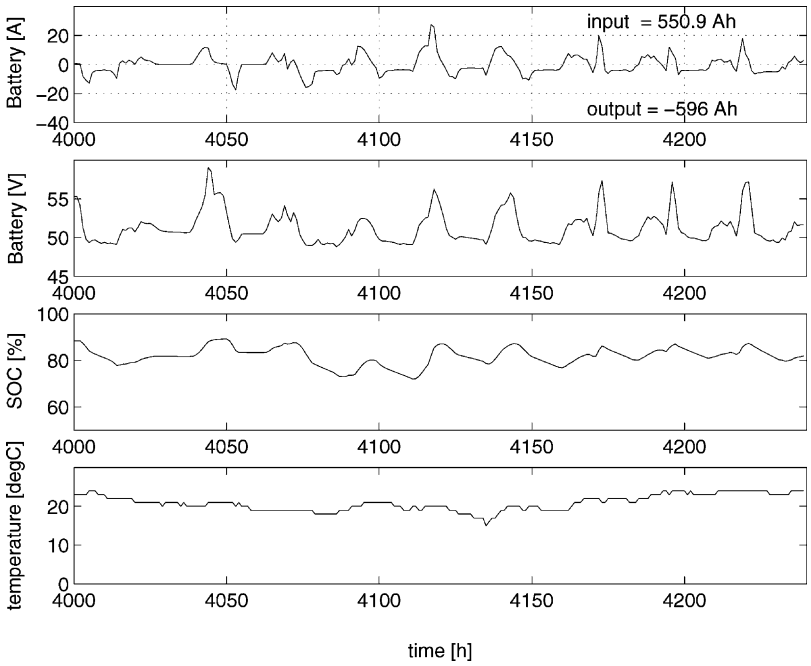

Fig. 11. Battery parameters for a 10-day period (TTA's 'mountain refuge' system).

Table 4
Summary results for the TTA 'mountain refuge' system, showing the additional throughput as a result of microcycles, at different load factors and ripple attenuation.

Ripple attenuation (%)	Load power factor	Total A h per year
100	1–0.6	14,452
0	1	15,859 (+10%)
0	0.6	19,220 (+33%)

throughput based on 1-h data underestimates the actual throughput, since the load current in particular is likely to be variable during the averaged measurement period.

The lifetime resulting from the temperature dependent corrosion process can be estimated from the standby lifetime (typically 12 years @ 20 °C), and the battery temperature profile measured in the application. It is generally accepted that an increase in temperature of 7–10 °C leads to a halving

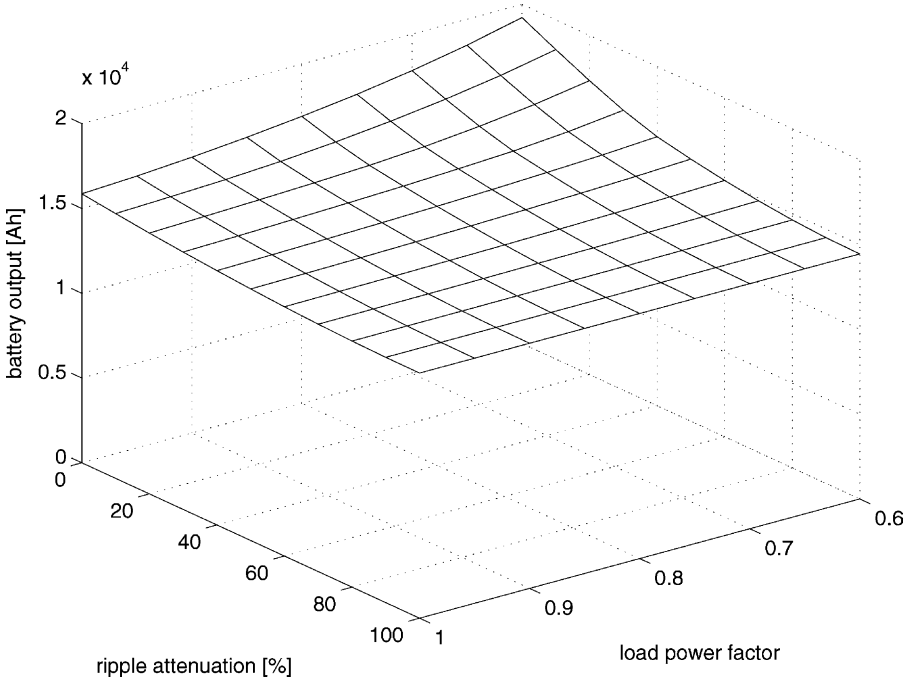

Fig. 12. Calculated total battery throughput for a period of 1 year (TTA's 'mountain refuge' system).

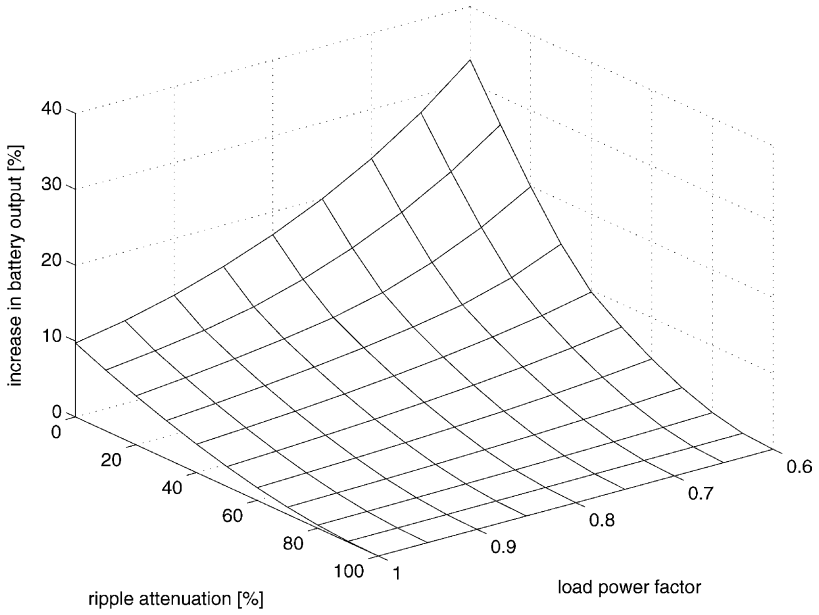

Fig. 13. Calculated increase in battery throughput resulting from microcycles caused by the load inverter (TTA's 'mountain refuge' system).

of the expected lifetime in float service. Although, temperatures of <20 °C would predict an increased lifetime, temperatures <20 °C are assumed to result in the same corrosion rate as at 20 °C, resulting in a conservative lifetime estimate. It was estimated that a factor of 0.8 should be included to account for the fact that the battery voltage is variable, and is not equal to the specified float voltage. In the 'mountain refuge' application, the predicted lifetime due to temperature-dependent corrosion was calculated to be 8.9 years.

Therefore, the limits to battery lifetime are likely to be the temperature-dependent corrosion process, and the effect of sulphation due to periods of operation at low SOC. This suggests that the battery wear due to increased microcycle throughput is not likely to be significant in this application, assuming that the mechanism causing this wear is similar to that for normal cycling. However in other classes of RES with higher battery throughput, where the battery lifetime is primarily determined by the cycling lifetime, microcycles are likely to reduce the battery lifetime.

4. The effects of microcycles

4.1. Experimental investigation of the effects of microcycles

Recent experimental work has been reported separately [7]. A special test equipment was built to investigate the effects of microcycles, capable of generating microcycles with a frequency up to 15 kHz, and with a maximum current of 200 A. The rate of current change is approximately 100 A μs^{-1} and the minimum duration of a current pulse is approximately 6 μs. This specification far exceeds the spectrum of currents normally encountered in a renewable energy system, although similar current amplitudes have been observed when occasional large loads, such as power tools, are connected. Although, high current pulses are required in order to conduct an accelerated test in a reasonable time period, high currents will increase the proportion of current contributed by charge-transfer relative to that supplied by the double layer capacitance. Therefore, the accelerated test is likely to produce more wear, as indicated by loss of capacity, than would be the case with the same throughput at lower currents.

Lead–acid cells were subjected to microcycles at different states of charge for 96 and 120 h, at frequencies ranging from 50 Hz to 8 kHz. Both symmetrical square pulses were used and also asymmetrical pulses to resemble a strong nonlinear load drawing mainly the third harmonic current at the ac side of the inverter. By means of a special control device the total throughput during these experiments was kept so small that no change of state-of charge can be caused by the microcycles. All the experiments showed an effect on either the capacity or the charging characteristics. The experiments with the most severe capacity loss were those without constant stirring of the electrolyte, but even with constant stirring of electrolyte a slight change of the charging characteristics was observed. Tests conducted on flooded lead–acid batteries with an acid agitation system showed no loss of capacity, while there was a small increase in charging time. The results of testing flooded lead–acid batteries without electrolyte agitation show that microcycles lead to increased acid stratification, and result in a progressive loss of battery capacity which is generally consistent with that caused by normal cycling. Some of this capacity loss is reversible under full recharge–discharge conditioning in the laboratory. In addition, the current and voltage profile during charging were found to be significantly changed, leading to

slower and inadequate charge using standard charge profiles. This behaviour is consistent with progressively increasing levels of irreversible sulphation.

4.2. Theoretical consideration of the effects of microcycles

Two processes seem to contribute to the effect of microcycling and can be used to explain them. They are specific aspects of the well-understood overall processes which cause reversible and irreversible ageing as a result of cycling and float operation.

4.2.1. Inhomogeneity of current density

The current distribution in electrodes is a complex function of the internal resistance of the grid, active material and electrolyte along the current path and the electrochemical polarisation at the site of the reaction. The electrochemical polarisation depends on the concentration of the involved ions, the deviation of the concentration of the ions from the equilibrium concentration and the specific current density and therefore the current and the available active surface. In lead–acid batteries, the concentration of the sulphuric acid electrolyte changes with the state-of-charge. This leads to changes in the ion concentrations and the electrical characteristics. This is different to other battery systems where the electrolyte is not consumed in the discharge reaction.

Acid stratification is caused by the internal resistance of the grids and electrodes and the effect of gravity. High density electrolyte will displace low density electrolyte underneath it. In the beginning of a discharge of a fully charged battery with homogeneous electrolyte, the electrodes are discharged more at the top of the electrode closer to the current collector, group bars and poles, initiating the development of acid stratification with an ultimately higher concentration at the bottom of the cell. The continued further development of acid stratification is complex because the electrochemical potentials due to differing acid concentrations results in a current distribution which partly compensates for the acid stratification. Once acid stratification has been caused by the discharging process, even if the gradient is only very small, the current distribution during charging and discharging is no longer the result of the internal resistance only, but also the result of the voltage difference between the equilibrium voltage at a specific reaction site and the charging or discharging voltage. The charging current density will be slightly higher at the top of the electrode than at the bottom and the discharging current density will be higher at the bottom of the electrode. As a result, the active material at the top will be increasingly charged, whereas the active material at the bottom will be increasingly discharged.

The process is well understood, and the onset of acid stratification is inevitable for cycling at partial state-of-charge without electrolyte agitation. It should be noted that batteries with immobilised electrolyte of the Gel or AGM type also develop acid stratification over long periods of time, however, other effects usually contribute more to ageing [15]. Experiments and model calculations for cycling batteries at a partial state-of-charge show that the unequal distribution of throughput of the electrodes is reduced if the current density is increased, and there is a more uniform current distribution in the case of higher currents [16].

The physical model describing the inhomogeneous current distribution after acid stratification has been generated is not sensitive to the duration of the charging and discharging periods. As long as the battery is in equilibrium, it can be expected that the results will also apply for shorter cycles. Indeed the experimental results are in line with these expectations. Experiments with electrolyte circulation show a much lower change in the battery performance due to microcycles because at all times the electrolyte density along the electrodes is uniform and therefore, the previous effect cannot exist. However, the current density distribution across the electrodes is also inhomogeneous. This phenomenon could be the cause of the change in the charging characteristics when using asymmetric charge/discharge pulses. The reason is a complex function of the electrolyte conductivity, the active mass conductivity and the electrochemical polarisations during the charging and the discharging reaction [16]. Further experiments need to be carried out to verify whether this model can explain the differences that are observed.

4.2.2. Effect on the microstructure

A number of different processes take place during either charging or discharging. During normal discharging, lead ions have to be formed in a dissolution process from the electrodes, a transfer of electrons has to take place and lead sulphate has to deposit on seed crystals of lead sulphate in the immediate vicinity of ion formation. Disregarding the voltage sag (‘cou de fouet’ effect) at the beginning of discharging, all of these processes are very quick and lead to the very fast response time of lead–acid batteries that make them so useful. Fast charge–discharge cycles (microcycles) will not necessarily result in a chemical conversion, because of the effect of the double-layer capacitance. The behaviour will be completely capacitive above certain frequencies (depending on the charge magnitude), with values stated by various researchers of the order of 1000 Hz. At lower frequencies, cyclic electrochemical processes take place. Due to the inhomogeneous current distribution as a result of different electrical resistances and electrochemical potentials, the formation of lead ions available for charging tends to take place in macroscopically different regions of the electrode to the formation of lead ions available for discharging. In our view, it is possible that this will lead to changes in the microstructure, however experimental evidence for this assumption does not yet exist.

The dependence of the size distribution of lead sulphate ions on the current density was recently investigated by Schattner [17]. During charging, small lead sulphate crystals

dissolve more quickly than large crystals because the ratio of surface area and volume is larger and the surface energy of small crystallites is more favourable for dissolving. During discharging, larger lead sulphate crystals provide a greater part of the total surface area available for deposition, and therefore will grow relatively faster than smaller ones. Microcycles will therefore shift the size distribution of lead sulphate crystals to larger crystals. Larger lead sulphate crystals should result in higher voltages during charging and a reduced charge efficiency, an effect which has been confirmed experimentally. The same basic considerations of a preferred deposition on larger crystallites and a preferred dissolution of smaller crystals, may also apply to some other processes involved during charging and discharging, for example, the structure of the lead dioxide material.

5. Conclusions

Conventional methods of analysis of the battery operating regime, and prediction of battery lifetime, are based on available mean data for solar irradiance and wind speed, typically measured at 10-min or 1-h intervals. The result is that short-term fluctuations and associated charge–discharge cycles are ignored, resulting in underestimation of battery throughput and associated wear. Additional cycling at 100 Hz caused by the operation of inverters directly from the battery, without dc–dc conversion, is a particular source of additional cycling. The effect of the additional throughput due to microcycles is likely to be most significant in system classes with operating conditions where the battery lifetime is mainly determined by wear rather than corrosion.

This paper proposes a method of analysis which takes into account the additional battery throughput due to microcycles caused by the generators and the load. It is found that the additional throughput caused by microcycles in batteries in renewable energy systems can be a significant proportion of the throughput estimated using mean data only. There is evidence that these microcycles might lead to a capacity loss and a lower state-of-charge under the operating conditions of renewable energy systems, which is likely to be caused by changes in the current distribution and the microstructure of the active materials.

The battery currents in typical Fraunhofer ISE classes 1 and 2 [5] renewable energy systems have been obtained by measurement and simulation. The main source of microcycles in the two systems studied was found to be a load inverter of the type operating directly off the battery without capacitive storage. The battery throughput was found to be increased by microcycles by as much as 76% (class 1 system), and by 33% (class 2 system). However even including the effect of microcycles, the battery throughput per year was rather low in both systems, being less than thirty times the nominal battery capacity. This is in contrast to class 3 or class 4 systems, where the battery throughput could be up to 200 times the battery capacity per year, and where the presence of microcycles is likely to be a significant factor in determining battery lifetime.

The inverter design is crucial to the reduction of battery current microcycles. It is recommended that a two-stage converter with capacitive energy storage is used in order to minimise ac battery currents, and reduce battery wear. Where possible, appliances connected to the ac supply should be designed to operate at near unity power factor. In addition, high frequency switching currents should be filtered as standard practice.

Acknowledgements

The work described in this paper was partly funded by the European Commission, Project number JOR3-CT98-0216.

References

[1] D.J. Spiers, A.D. Rasinkoski, Predicting the service lifetime of lead/acid batteries in photovoltaic systems, J. Power Sources 53 (2) (1995) 245–253.
[2] D.J. Spiers, A.A. Rasinkoski, Limits to battery lifetime in photovoltaic applications, J. Solar Energy 58 (4-6) (1996) 147–154.
[3] S. Drouilhet, B.L Johnson, A battery life prediction method for hybrid power applications, in: Proceedings of the Presentation of Collection of the 1997 ASME Wind Energy Symposium Technical Papers at the 35th AIAA Aerospace Sciences Meeting and Exhibition, Reno, Nevada, 6–9 January 1997, pp. 149–159.
[4] P.C. Symons, Life estimation of lead–acid battery cells for utility energy storage, in: Proceedings of the Fifth International Conference on Batteries for Utility Storage, San Juan, Puerto Rico, July 1995.
[5] D.U. Sauer, M. Bächler, G. Bopp, W. Höhe, J. Mittermeier, P. Sprau, B. Willer, M. Wollny, Analysis of the performance parameters of lead/acid batteries in photovoltaic systems, J. Power Sources 64 (1997) 179–201.
[6] H. Wenzl, C. Ropeter, E.A. Wehrmann, G. Bopp, D.U. Sauer, A.G. Dutton, A.J. Ruddell, J. Merten, C. Orfanogiannis, J.W. Twidell, P. Vezin, Microcycles in batteries of renewable energy remote power systems, in: Proceedings of the Sixth International Conference on Batteries for Utility Energy Storage, Gelsenkirchen, Germany, 21–23 September 1999.
[7] C. Ropeter, H. Wenzl, H.P. Beck, E.A. Wehrmann, J.W. Twidell, D.U. Sauer, The impact of microcycles on batteries in different applications, in: Proceedings of the 18th Electric Vehicle Symposium (EVS18), Berlin, 20 October 2001.
[8] A.I. Harrison. Batteries and ac phenomena in UPS systems, INTELEC89, in: Proceedings of the 11th International Telecommunications Energy Conference, Florence, Italy, October 1989.
[9] F. König, Der Einfluß von Wechselstrom auf Bleibatterien (The influence of alternating current on lead batteries), ETZ-B 16 (18) (1964) 536.
[10] L.T. Lam, H. Ozgun, O.V. Lim, J.A. Hamilton, L.H. Vu, D.G. Vella, D.A.J. Rand, Pulsed-current charging of lead/acid batteries—a possible means for overcoming premature capacity loss? J. Power Sources 53 (2) (1995) 215–228.
[11] S. Ozazaki, S. Higushi, O. Nakamura, S. Takahashi, Influence of superimposed alternating current on capacity and cycle life for lead–acid batteries, J. Appl. Electrochem. 16 (1986) 894–898.
[12] R. Kaushik, I.G. Mawston, Coulombic efficiency of lead–acid batteries, particularly in remote-area power-supply (RAPS) systems, J. Power Sources 35 (1991) 377–383.

[13] J.B. Copetti, E. Lorenzo, F. Chenlo, A general battery model for PV system simulation, Prog. Photovoltaics: Res. Appl. 1 (1993) 283–292.

[14] J.W. Stevens, G.P. Corey, A study of lead–acid battery efficiency near top-of-charge and the impact on PV system design, in: Proceedings of the 25th IEEE Photovoltaic Specialists Conference, Boston, USA, May 1996, pp. 1485–1488.

[15] Döring et al., PV-Betrieb und Fehlermodus verschiedener Speicherbatterien und Empfehlungen für die Betriebsführung (PV operation and types of fault of different storage batteries and recommendations), in: Proceedings of the 10th Symposium Photovoltaische Sonnenenergie, Staffelstein, Germany, 1995.

[16] D.U. Sauer, J. Garche, Optimum battery design for applications in photovoltaic systems—theoretical considerations, J. Power Sources 95 (1-2) (2001) 130–134.

[17] S. Schattner, Reversible Kapazitätsentwicklung von Bleibatterien bei Belastung mit wechselstromhatligen Gleichsträömen (Reversible development of capacity of lead–acid batteries under dc currents with ac ripple), Final year thesis, Universität Karlsruhe Elektrotechnische Institut and Fraunhofer Institut für Solare Energiesysteme, 1997.